Untraditional Approach to Complex Hierarchical Periodic Arrays with Trinary Stepwise Architectures of Micro-, Submicro-, and Nanosized Structures Based on Binary Colloidal Crystals and Their Fine Structure Enhanced Properties

Yue Li,[†,‡,*] Naoto Koshizaki,[‡,*] Hongqiang Wang,[‡] and Yoshiki Shimizu[‡]

[†]Key Laboratory of Materials Physics, Anhui Key Laboratory of Nanomaterials and Nanotechnology, Institute of Solid State Physics, Chinese Academy of Sciences (CAS), Hefei 230031, Anhui, China, and [‡]Nanosystem Research Institute (NRI), National Institute of Advanced Industrial Science and Technology (AIST), Central 5, 1-1-1 Higashi, Tsukuba, Ibaraki 305-8565, Japan

ABSTRACT

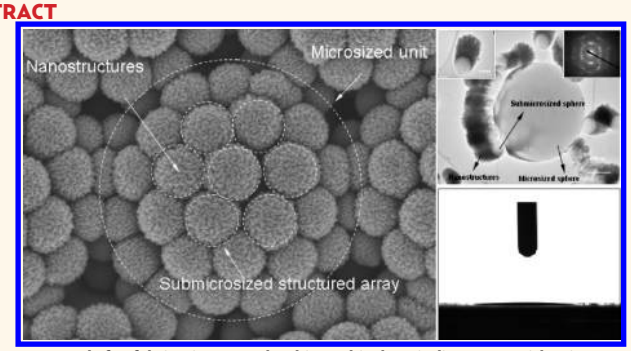

A unique approach for fabricating complex hierarchical periodic arrays with trinary stepwise architectures of micro- and submicro- as well as nanosized structures by combining a novel double-layered binary colloidal crystal with pulsed laser deposition techniques is developed. The present strategy is universal and nanostructures with different materials can be easily prepared in the complex hierarchical periodic arrays. This approach offers the advantage of low costs compared to conventional lithographic techniques. These as-prepared unique structures cannot be directly fabricated by conventional lithography. These special hierarchically structured arrays demonstrate fine structure-enhanced performances, including superhydrophilicity without UV irradiation and surface enhanced Raman scattering (SERS), which is highly valuable for designing micro/nanodevices, such as biosensors or microfluidic devices.

KEYWORDS: hierarchical array · trinary · binary colloidal crystals · enhanced properties

Hierarchical micro/nanostructures possess unique properties and offer the advantages of both microsized structures and nanostructures and therefore have many applications in optoelectronic devices, microfluidic devices, biomedical science, field emission, *etc.*[1−5] If these hierarchical structures can be arranged into ordered arrays, this will further improve applications in micro/nano-devices because of their more stable and uniform properties on the array surfaces.[3−5] Generally, hierarchical structures could be synthesized by replication induced by an electric field, chemical vapor deposition, or electron irradiation.[6−10] Unfortunately, it is difficult to cause them to form ordered arrays by self-assembly due to limitations of the geometric configuration once the hierarchical structures have been prepared. Conventional approaches to hierarchical micro/nanostructured arrays are generally based on lithographical techniques. Microsize-structured arrays are first fabricated by lithography, including photolithography, X-ray lithography, e-beam lithography, *etc.*[11−14] and then nanosized structures are created based on the microsized ones.[15] Thus, hierarchical micro/nanostructured arrays can be achieved. However, an approach based on traditional lithography can only be afforded by a few laboratories due to the low sample throughput and high cost, hindering further applications of the special structured arrays. More importantly, one hardly devises and manufactures more complex hierarchical arrays by such an approach. Therefore, an unconventional approach to create micro- or nanosized arrays has attracted much attention, and it is urgent to develop a new technique for fabricating complex hierarchically structured arrays to overcome the above disadvantages.

* Address correspondence to yueli@issp.ac.cn, koshizaki.naoto@aist.go.jp.

Received for review March 2, 2011 and accepted October 28, 2011.

Published online October 29, 2011
10.1021/nn203239n

It has been proven that the monolayer colloidal crystal template technique is an efficient approach to micro- or nanostructured patterns including particle arrays, pore arrays, and ring arrays, *etc.*[16−23] If one chooses a colloidal monolayer with microsized spheres and then deposits nanomaterials (*i.e.*, nanoparticles, nanotubes, and nanorods), the desired hierarchical micro/nanostructured arrays will be easily obtained.[24−27] However, more complicated hierarchically structured arrays are required in some cases for special applications in biotechnology or other fields. It is crucial to design and create complex hierarchically structured arrays featuring low cost and facile manipulation. On the basis of the colloidal monolayer templates, although various periodic patterns have been developed, it is still difficult to devise more complex hierarchical structured arrays due to the simple, general hcp alignment of their colloidal monolayer. With development of the colloidal assembling technique, more complex colloidal crystals, such as binary colloidal crystals, can be fabricated by spin coating,[28] dip coating,[29−32] horizontal deposition,[33−36] and coself-assembly at the air−water interface,[37,38] where small colloidal spheres were filled in the interstices of colloidal crystals according to certain rules. The success of binary colloidal crystals might bring a greater chance to achieve more complicated hierarchical structured arrays in combination with other techniques.

We present a novel approach to prepare complex hierarchical periodic arrays with microsize, submicrosize, and nanosize trinary stepwise structures based on a double layered binary colloidal crystal with different sphere sizes in each layer. Such a hierarchical binary colloidal crystal was obtained by float-transferring the second-layered colloidal monolayer with submicrosized spheres onto the first layered colloidal monolayer with microsized spheres that was prefixed on the substrate. Such binary colloidal crystals possess the advantages of original hcp alignments for both bottom and top layers of colloidal crystals, which is quite different from previous reports.[28−38] Finally, the nanostructured materials were created on the hierarchical colloidal crystals by pulsed laser deposition (PLD). Herein, CuO deposition was used as an example to demonstrate the fabricating process of such complex structured arrays. We successfully obtained complex hierarchical periodic arrays with trinary stepwise architectures of micro-, submicro-, and nanosized structures by this strategy, and such complex hierarchical periodic arrays demonstrated fine structure-enhanced performance, that is, superhydrophilicity without UV irradiation. Generally, superhydrophilicity could be created by increasing the surface roughness of materials with high free energy according to the Wenzel model.[39] The superhydrophilicity demonstrated by such complex hierarchical periodic arrays should be attributed to their rough enough surfaces and the PLD process. Besides superhydrophilicity, such a complex hierarchical array after being coated with a thin gold layer also exhibited an excellent surface-enhanced Raman scattering (SERS) effect for detecting organic molecules when it was used as an active substrate of SERS. Additionally, the feature of hierarchical ordered arrays with trinary stepwise architectures was almost kept after the removal of the binary colloidal crystal by the annealing process, and microsized and submicrosized holes were templated by the double-layered binary colloidal crystals. More importantly, it is almost impossible to create such complex hierarchical arrays by traditional lithographical techniques. Such specially structured arrays have highly valuable applications in optical, biotechnical, separation science, and microfluidic devices as well as bionic devise.

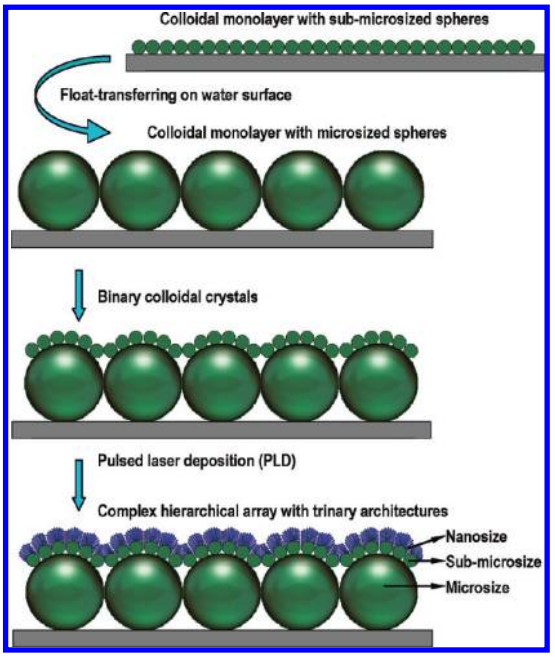

Scheme 1. Schematic illustration of the fabrication process for a complex hierarchical periodic array with trinary stepwise architectures.

In this approach, a colloidal monolayer composed of large spheres (microsized PS spheres: 2 or 5 μm) was first fabricated on a cleaned Si or glass substrate by interface self-assembly as Giersig M. *et al.* described,[40−42] and this monolayer was fixed onto the substrate by heating it at 120 °C for 3 min. The fixed colloidal monolayer on the substrate was treated by ozone cleaner in order to make its surface hydrophilic to guarantee the subsequent transferring of another colloidal monolayer. Another colloidal monolayer with small spheres (submicrosized PS spheres: 350 or 200 nm) prepared on another substrate was slowly dipped into water. It was then gradually peeled off from the substrate and floated on the water surface. A binary colloidal crystal of double layers with micro-/submicrosized structures was thus

obtained by picking up the colloidal monolayer with small spheres from the water surface using the colloidal monolayer with large spheres prefixed to the substrate. Finally, nanostructures were created on the colloidal double layers by pulsed laser deposition (PLD). Complex hierarchical ordered arrays with trinary stepwise structures of micro-, submicro- and nanosize were obtained, as schematically illustrated in Scheme 1.

RESULTS AND DISCUSSION

Morphology and Structure. Figure 1 presents SEM images of typical hierarchically structured arrays with trinary stepwise architectures using CuO as a target in the PLD process. One can see that these special structured arrays possess micro-, submicro-, and nanosized structures. A microsized structure with a size of 2 μm exhibited a hexagonal close-packed (hcp) arrangement, as seen in Figure 1A. Each microsized unit was composed of hcp-aligned submicrosized structures with a size of 350 nm, and each submicrosized unit consisted of nanostructures with sharp tips (Figure 1B). From the cross-sectional FE-SEM image, the microsized structure unit is reflected from the microsized PS colloidal sphere, and the submicrosized structure unit is reflected from the submicrosized PS sphere on the microsized sphere. The nanostructures on the submicrosized PS spheres were formed by the PLD process. We can also observe that the spheres at the bottom of the colloidal layer had a contact area with the substrate or with each other (Figure 1C), caused by heating deformation when the colloidal monolayer was heated slightly above the PS glass transition temperature (T_g).[43−45] The contact between sphere and substrate or between two neighboring spheres guaranteed that the colloidal monolayer was well fixed on the substrate and it could not be peeled off from the substrate during the subsequent transfer of a second colloidal monolayer in water. The microsized colloidal sphere layer at the bottom was fabricated by a self-assembling approach at the interface of air and water, which produced the typical hcp arrangement, finally resulting in an hcp structure in the hierarchical structures. The second submicrosized sphere colloidal monolayer was obtained on a substrate using the same approach and then transferred onto a microsized colloidal layer supported on the substrate, while maintaining its integrity and hence also the hcp alignment. Nanostructures with columnar structures were formed by PLD on the top of submicrosized spheres in the second layer of the final hierarchical arrays. The column-like nanostructures deposited on the second colloidal monolayer were caused by both the shadow effect and multidirectional deposition at the high pressure of the background gas in the PLD process.[46]

The X-ray photoelectron spectroscopy (XPS) survey spectrum indicates that the materials deposited by

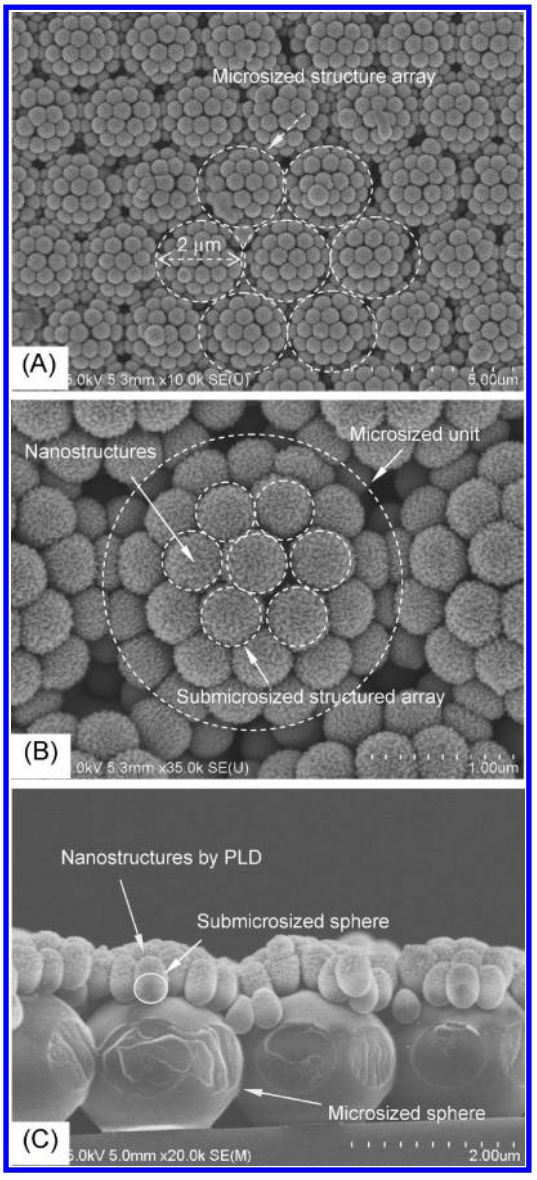

Figure 1. FE-SEM images of CuO periodic arrays with ternary stepwise hierarchical structures of micro-, submicro-, and nanosize: (A, B) top view image; (B) magnified image of one unit from image A; (C) cross-section image.

PLD are composed of Cu and O from the CuO target (Supporting Information, Figure S1). The XRD spectrum (Supporting Information, Figure S2) further indicates that the materials are crystalline CuO with a much higher relative intensity of the (002) peak compared with the standard data for bulk CuO (JCPDS 801268), suggesting that the deposited CuO nanostructures are well aligned and have a preferential orientation along the *c*-axis, attributable to a template-induced fabrication effect. A similar orientation has also been observed in a lithography-induced growth process.[47−49]

A typical TEM image of a complex, hierarchical trinary structured unit is presented in Figure 2. It can clearly be seen that the structure is composed of microsized and submicrosized spheres and nanostructure on a submicrosized sphere surface, which agrees

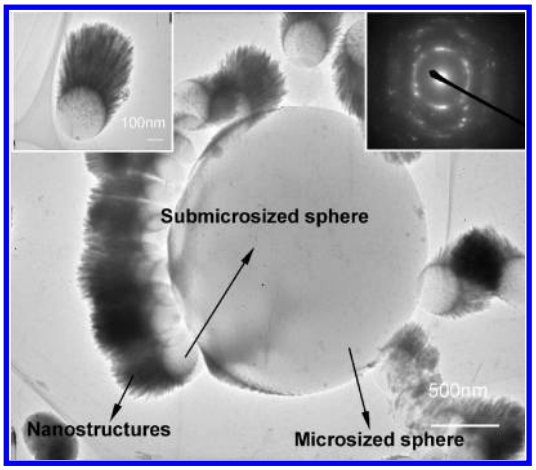

Figure 2. TEM image of a unit in an as-prepared trinary stepwise structured array. Inset at the left top is a submicrosphere with nanostructures peeled off from the trinary structure unit. Inset on the right top is the selected area electron diffraction (SAED) pattern of the nanostructures deposited by PLD.

with the SEM sectional image of the sample. The separated nanostructures with their supporting small PS spheres display radially aligned nanorod structures with sharp tips that grow almost vertically on the small PS sphere surface (inset on the left top). The selected area electron diffraction (SAED, inset on the right top) pattern demonstrates that the nanorods deposited on the small PS spheres by PLD are polycrystalline CuO, coinciding well with the XRD result.

In the presented strategy, complex trinary stepwise architectures with micro-/submicro- /nanostructures can be tuned by changing the periodicities of the bottom colloidal monolayer and the second colloidal crystal, as well as by changing the deposition conditions during the PLD process (*e.g.*, the background gas pressure and deposition time). For instance, by simply changing the PS sphere size for the second-layer colloidal crystal from 350 to 200 nm without any other alteration of the fabrication process, a similar complex hierarchically structured array with the same microsized and nanosized structures but different submicrosized structures was obtained, as depicted in Figure 3A. If we changed the periodicity of the bottom colloidal monolayer from 2 to 5 μm, we could also achieve a similar hierarchical array with the submicrosized and nanosized structures unchanged (Figure 3B). If the periodicities of both the bottom and second colloidal layers were changed, a similar complex hierarchically structured array can also be created (Figure 3C). The nanostructures could be usually tuned by changing the background gas pressure and deposition time.

Additionally, we found that morphologies of such hierarchical structured arrays with trinary stepwise architectures with micro-/submicro-/nanostructures could be almost inherited from the former ones after being annealed at high temperature in ambient air;

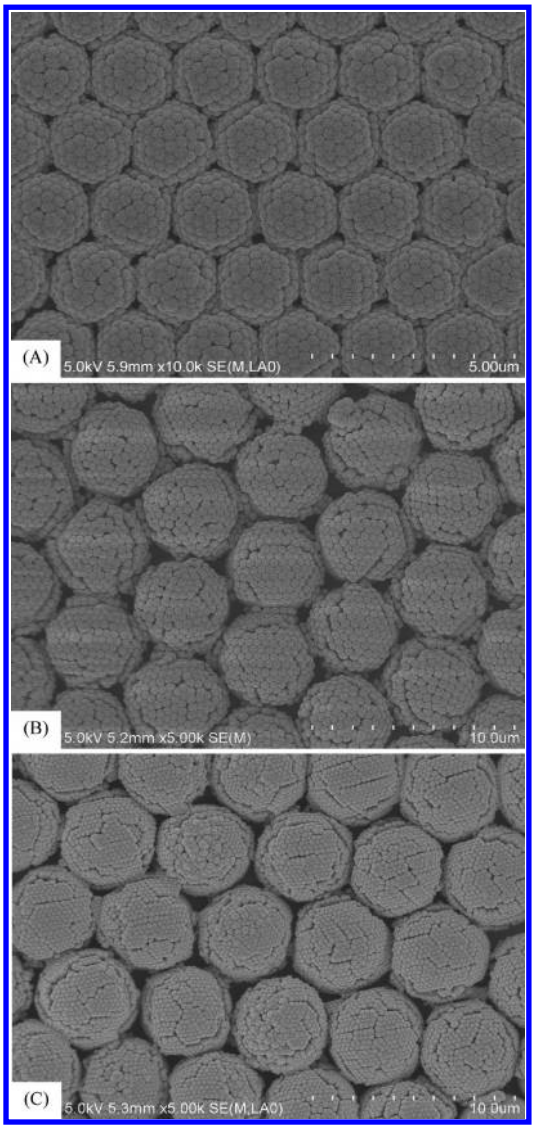

Figure 3. Hierarchical periodic structured arrays based on double layered binary colloidal crystals with variable microsized and submicrosized PS sphere. Microsize/submicrosize: (A) 2 μm/200 nm; (B) 5 μm/350 nm; (C) 5 μm/200 nm.

even the binary colloidal crystal was removed due to pyrolysis of PS in the annealing process. Herein we present in Figure 4 the CuO hierarchical trinary structured arrays based on the binary colloidal crystal of 2 μm/350 nm after annealing. The microsized units in the hierarchical array still kept the hcp alignment, and the submicrosized units on the spherical surface of the microsized unit also kept the hcp pattern. However, the nanostructures were a little bit different from those before annealing. After being annealed, the nanostructures changed from radially aligned nanorods with sharp tips to spherical nanoprotuberances on the submicrosized unit surface (insets in Figure 4A), which originate from the atomic diffusion of the nanomaterials with sharp tips in the annealing process. Additionally, it was discovered that microsized holes and submicrosized ones were formed under hierarchical trinary

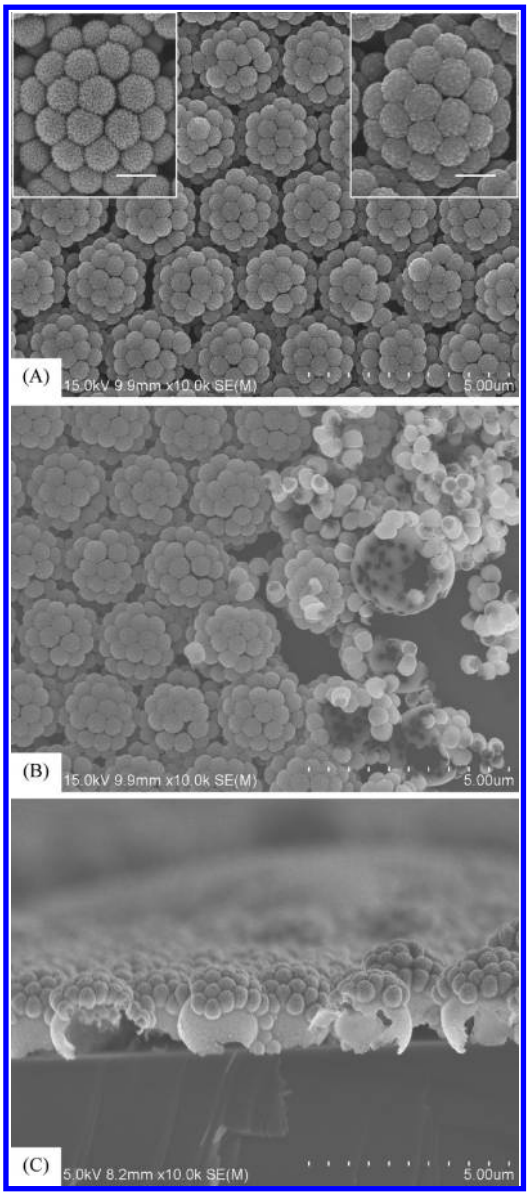

Figure 4. CuO hierarchical structured array with trinary stepwise architectures after annealing at 600 °C for 3 h in ambient air. Microsized sphere/submicrosized sphere: (A) 2 μm/350 nm, low magnification FE-SEM image; left and right inset in panel A shows FE-SEM images with high magnification before and after annealing, respectively. Scale bars in inset: 500 nm; (B) damaged sample scraped by tweezers; (C) cross-section image.

stepwise arrays (Figure 4B), which templated from binary colloidal crystals in the annealing process. The cross section image demonstrated that CuO walls were also created on the microsized PS sphere surface in PLD (Figure 4C), which supported the whole hierarchical structured arrays on the substrate after removal of the PS templates by pyrolysis of PS. The hierarchical array film adhered tightly to the substrate after annealing and could not be detached from the supporting substrate even when it was ultrasonicated in water for 20 min. The hierarchical periodic array with hierarchical holes with microsized and submicrosized structures has important applications in separation science.

The proposed strategy is universal for creating such special hierarchical structured arrays by changing the target to various materials in the PLD process. Besides CuO, other materials such as ZnO, Fe_2O_3, TiO_2, NiO, WO_3, SnO_2, and C with similar hierarchical micro-/submicro-/nanostructured arrays can be fabricated. Figure 5 presents a polycrystalline-structured ZnO (Figure 5A,B) and Fe_2O_3 (Figure 5C,D) array with trinary hierarchical architectures obtained by PLD on a binary colloidal crystal using ZnO and Fe_2O_3 as targets (oxygen pressure, 6.7 Pa; deposition time, 0.5 h for ZnO and 1 h for Fe_2O_3). Figure 5 panels E and F depict amorphous TiO_2 micro-/submicro-/nanostructured arrays by the same approach, using TiO_2 as a target at 6.7 Pa oxygen pressure for 40 min deposition time. Additionally, we clearly observed that fine nanostructures of ZnO, Fe_2O_3, and TiO_2 were slightly different, which could be mainly resulted from their various chemical and physical properties, such as crystal facets of the interface with different energies.

Fine Structures Enhanced Properties. *Superhydrophilicity without UV Irradiation.* These special hierarchical micro-/submicro-/nanostructured arrays exhibit certain structure-enhanced properties due to their unique structures. For example, CuO hierarchically structured arrays with trinary architectures without annealing exhibited superhydrophilicity without UV irradiation and the water contact angle (CA) was 5.2°, as shown in Figure 6a. (Superhydrophilicity is usually defined as occurring when the water CA is less than 10° on the material surface and it is generally achieved by UV irradiation on semiconductor films.[50,51]) This superhydrophilicity was mainly induced by its special structures. Such superhydrophilicity is highly useful for devising the microfluidic devices and self-cleaning surfaces. A CuO nanoparticle film was also created by PLD on a flat substrate without using any PS sphere colloidal monolayer, under the same experimental conditions as for the hierarchically structured array with trinary architectures. The water CA of the nanoparticle film was 22.9° (Figure 6b). Hierarchically structured arrays with binary hierarchical structures were obtained by combining a colloidal monolayer with the PLD technique. The water CAs for binary hierarchically structured arrays based on a colloidal monolayer with PS sphere sizes of 350 nm and 2 μm were 19.2° and 15.3°, as seen in Supporting Information, Figure S3. Generally, the Wenzel mode is used to explain the wettability for a rough surface, where a water drop has complete wetting on it.[39]

$$\cos\theta_r = r\cos\theta \quad (1)$$

Here, r is the surface roughness, which is the ratio of the total surface area to the projected area on the horizontal plane, and θ_r and θ are the CAs of a particle film and a

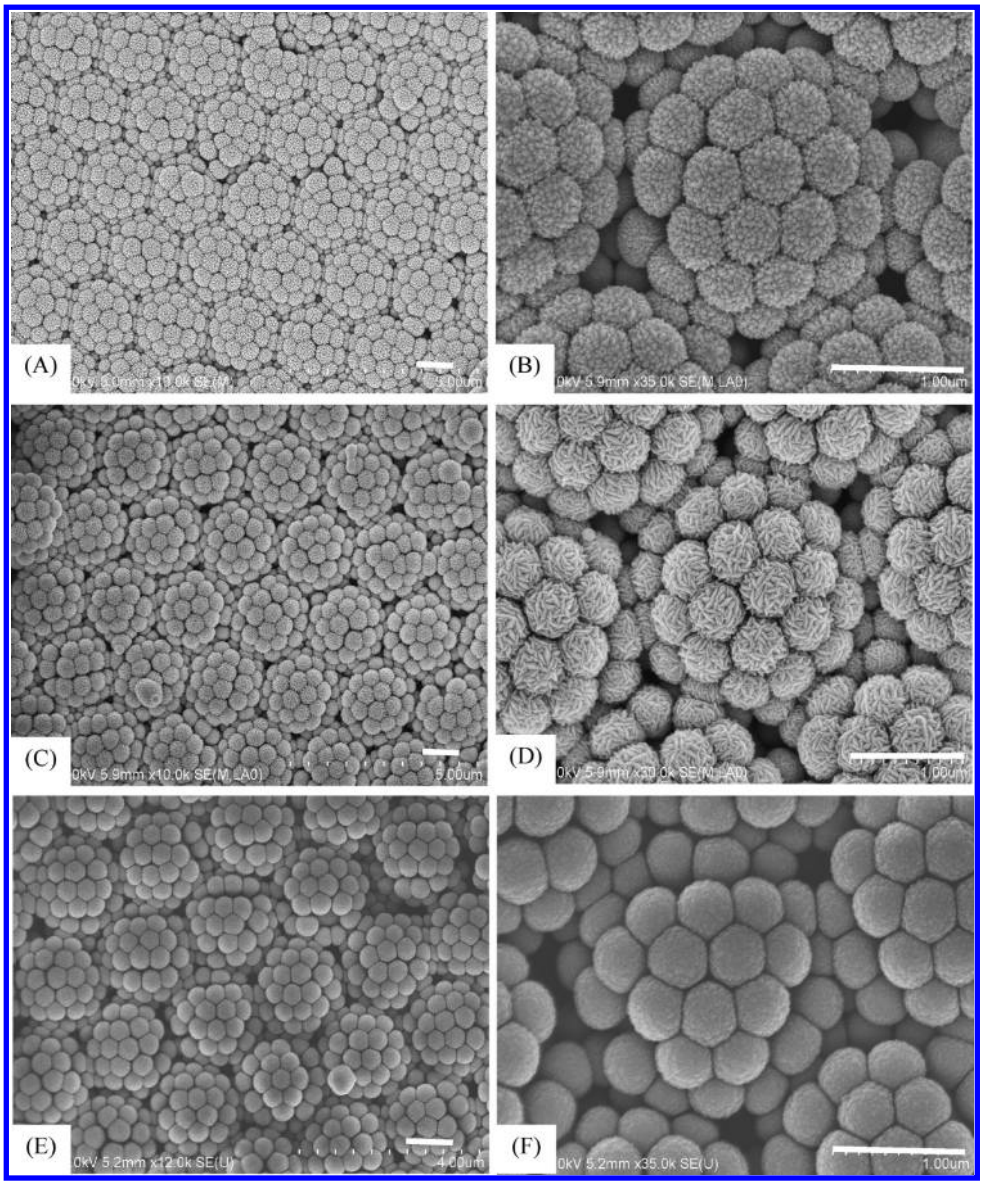

Figure 5. FE-SEM images of complex hierarchical micro-/submicro-/nanostructured arrays of ZnO, Fe_2O_3, and TiO_2 fabricated by the proposed strategy. (A, B) ZnO; (C, D) Fe_2O_3; (E, F) TiO_2. Scale bars are 1 μm.

smooth native film. This equation indicates that the wettability will be enhanced by increasing the surface roughness. Compared with the CuO film on a flat substrate produced by PLD without using any colloidal monolayers, the binary hierarchical micro-/nanostructured or submicro-/nanostructured array increased the roughness of the CuO surfaces, thereby enhancing the wettability while decreasing the water CA. However, the roughness is not enough to induce the surface wettability to superhydrophilicity. The special hierarchical micro-/submicro-/nanostructured arrays based on the binary colloidal monolayer greatly increase the surface roughness, leading to superhydrophilicity according to eq 1. Therefore, such superhydrophilicity without UV irradiation originated from fine structure enhanced properties and special process of PLD.

Active SERS Substrate. Such special hierarchical micro-/submicro-/nanostructured arrays with 10 nm Au coating exhibited excellent SERS effects using the R6G as a probe molecule (Curve e in Figure 7). For comparison, SERS performances of different substrates with the same Au coatings including smooth silicon wafer, CuO film by PLD without using colloidal monolayer (sample in Supporting Information, Figure S3A), hierarchical submicro-/nanostructured arrays produced by PLD using a colloidal monolayer with 350 nm PS spheres (sample in Supporting Information, Figure S3B) as well as micro-/nanostructured arrays produced by PLD using a colloidal monolayer composed of 2 μm PS spheres (sample in Figure S3C), were also investigated, as shown in Figure 7. Smooth Au coating on Si substrate only produced very weak SERS signal (curve a in Figure 7). The CuO film by PLD without using the

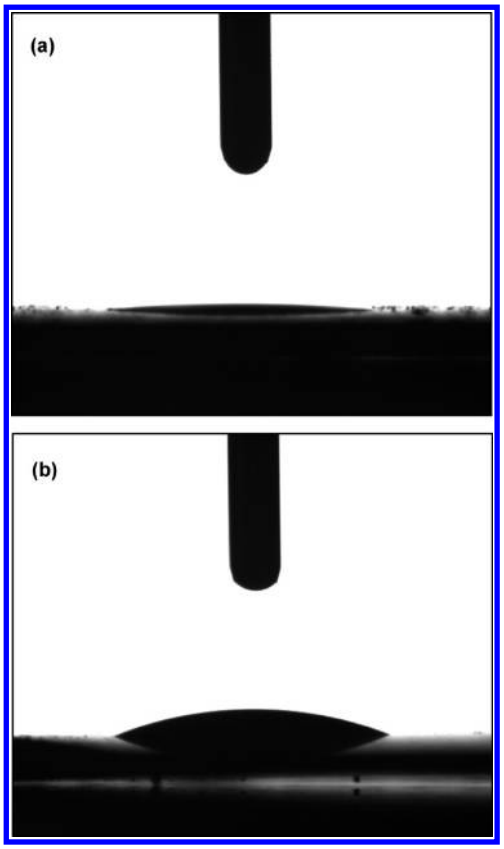

Figure 6. (a) Structure-enhanced wettability of hierarchical trinary stepwise structured arrays fabricated by using microsize spheres of 2 μm and submicrosize spheres of 350 nm by PLD without annealing, showing a water CA of 5.2°. (b) Water CA on a thin film on the silicon substrate obtained directly by PLD without using colloidal templates: water CA, 22.9°.

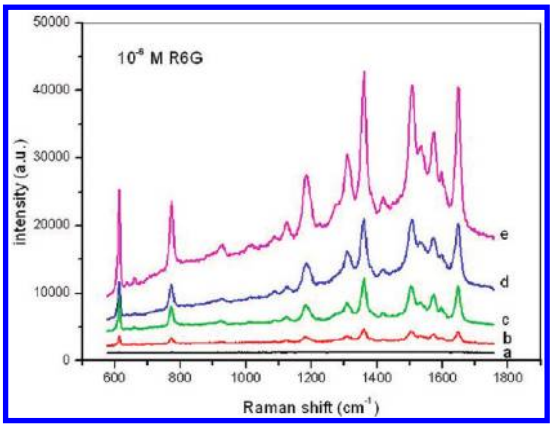

Figure 7. SERS spectra of R6G on different substrates after being coated with 10 nm gold layer: (a) smooth silicon wafer. (b) CuO film by PLD without using colloidal monolayer; (c) hierarchical micro-/nanostructured arrays produced by PLD using a colloidal monolayer with PS sphere sizes of 2 μm; (d) hierarchical submicro-/nanostructured arrays produced by PLD using colloidal monolayer with PS sphere sizes of 350 nm; (e) complex hierarchical trinary stepwise structured arrays with micro-/submicro-/nanosized units.

colloidal monolayer shows a stronger SERS property due to its relatively rough surface (curve b in Figure 7). The hierarchical micro-/nano- or submicro-/nanostructured array by PLD using colloidal monolayers with different PS sphere sizes (PS sphere size: 2 μm, 350 nm) as templates show much stronger signals owing to their rougher surfaces with two-scaled structures (curve c and d in Figure 7). Interestingly, the complex trinary micro-/submicro-/nanostructured array by PLD using binary colloidal crystal demonstrate dramatically increasing SERS property compared with the above four cases.

Generally, SERS performance is determined by matter and morphology of substrates.[52−54] Noble metals (*i.e.*, Au) are excellent candidates for SERS matter with rough surfaces. The sharp protrusion and gaps in nanoscale in a rough metallic matter surface will produce much larger electromagnetic enhancement at these sites, and therefore the intensity of the Raman spectra of the molecule absorbed on metal surfaces can be dramatically enhanced. So the rough structure units are usually called active "hot" spots, which could be mainly attributed to SERS properties.[55,56] The as-prepared complex hierarchical arrays with trinary stepwise architectures of micro-/submicro-/and nanosized structures possess many active "hot" spots for SERS-detecting organic molecules after coating the Au thin layer, which mainly contributes to their excellent SERS performances. From the CuO film directly by PLD, to hierarchical micro-/nano- or submicro-/nanostructured structured arrays by PLD based on colloidal monolayers, and finally to complex trinary micro-/submicro-/nanostructured arrays by PLD using binary colloidal crystals, the roughness of their surfaces increases, which leads to increasing active "hot" spots by SERS effect, finally resulting in the dramatical increase of the SERS signal. Besides increasing surface roughness, the feature of array periodicity also contributes to the excellent SERS effect to some extent. The periodic structures may produce the redistribution of the photon density of states, which leads to an increase of density of optical modes and thus the enhancement of the Raman scattering of the detected organic molecules. This fact has been proven by experiments and theoretical calculations.[57−59]

CONCLUSION

In summary, a unique approach to fabricating complex hierarchical periodic arrays with trinary architectures of micro- and submicro- as well as nanosized structures, developed by combining a double layered binary colloidal crystal with PLD techniques before and after annealing is presented. The strategy is universal and nanostructures with different materials could be easily prepared in the complex hierarchical periodic arrays. Compared to conventional lithographic techniques, this approach offers the advantage of low cost. Importantly, these unique structures cannot be fabricated by conventional lithography. These special hierarchically

structured arrays demonstrate structure-enhanced performances, including superhydrophilicity without UV irradiation and excellent SERS for detecting organic molecules. Additionally, such hierarchical trinary stepwise structured arrays with hole-architectures could be obtained after removal of the PS binary colloidal template by use of the annealing process, which has important applications in separation science. Overall, this strategy is highly valuable for designing micro-/nanodevices, such as biotechnological or microfluidic devices, based on these special structured arrays.

MATERIALS AND METHODS

A 2.5 wt % colloidal suspension with microsize (2 μm, 5 μm) or submicrosize (350 nm, 200 nm) monodispersed PS spheres was purchased from the Alfa Aesar Co. First, monolayer colloidal crystals with microsized PS spheres were fabricated on cleaned Si substrates by self-assembly at the interface between air and water and subsequent formation on the cleaned Si substrate after complete evaporation of the water, as previously described.[40−42] The microsized PS sphere colloidal monolayer was heated at 120 °C (slightly higher than the PS glass transition T_g = 100 °C) for 3 min in order to tightly fix it to the substrate and then was treated by ozone cleaning for 45 min to make a good hydrophilic surface. A submicrosized PS sphere monolayer was fabricated using the same approach without heating that gradually floated to the water surface. It was then picked up by the microsized PS sphere monolayer fixed on the substrate, and thus a double-layered binary colloidal crystal was formed with the bottom of the microsize PS sphere monolayer and the top of the submicrosize sphere layer on the substrate.

The double-layered binary colloidal crystal, on its supporting substrate, was placed in a chamber for PLD in an off-axis configuration. A laser beam with a wavelength of 355 nm from a Q-switched Nd:YAG laser (Continuum, Precision 8000) operated at 10 Hz with 100 mJ pulse^{-1} and a pulse width of 7 ns, was applied and focused on the target surface with a diameter of 2 mm. The target could be changed for different materials (CuO, Fe_2O_3, ZnO, or TiO_2). The substrate and target were rotated at 40 and 30 rpm. The PLD was carried out for different times at a base pressure of 2.66 $\times$ 10^{-4} Pa and a background O_2 pressure of 6.7 Pa for CuO, or at other suitable pressures depending on the deposited materials.

The water CA was measured with a VCA Optima XE from AST Products, Inc.

Previous to the investigation of the SERS spectra, all the samples were coated with 10 nm of a gold layer on their surfaces by sputtering. The samples with gold coating were dipped in the 10^{-6} M rhodamine 6G (R6G) aqueous solution for 10 min, and then rinsed with pure water and dried by nitrogen flow. The SERS properties were examined by a confocal microprobe Raman system (Renishaw inVia Raman Microscope). The excitation wavelength was 532 nm. The data integration time was 5 s, and five different positions were measured at each sample.

The morphologies of the as-prepared samples were observed using an FE-SEM (Hitachi S-4800) and a TEM (JEOL JEM-2000FX). The composition and chemical state of the samples were examined using X-ray photoelectron spectroscopy (XPS, PHI 5600ci). The water CA was measured with a VCA Optima XE from AST Products, Inc.

Acknowledgment. We are grateful to J. Wang, G. Duan from the Institute of Solid State Physics, CAS for experimental assistance in SERS measurements and for helpful discussions. This work was partially supported by the National Natural Science Foundation of China (Grant No. 10974203), and Anhui Provincial Natural Science Funds for Distinguished Young Scholar (Grant No. 1108085J20).

Supporting Information Available: XPS spectrum (Figure S1) and XRD pattern (Figure S2) of the sample after PLD of CuO and schematic illustration of water CAs on different surfaces (Figure S3). This material is available free of charge *via* the Internet at http://pubs.acs.org.

REFERENCES AND NOTES

1. Morariu, M.; Voicu, N.; Schäffer, E.; Lin, Z.; Russell, T. P.; Steiner, U. Hierarchical Structure Formation and Pattern Replication Induced by an Electric Field. *Nat. Mater.* **2003**, *2*, 48–52.
2. Li, Y.; Fang, X.; Koshizaki, N.; Sasaki, T.; Li, L.; Gao, S.; Shimizu, Y.; Bando, Y.; Golberg, D. Periodic TiO_2 Nanorod Arrays with Hexagonal Nonclose-Packed Arrangements: Excellent Field Emitters by Parameter Optimization. *Adv. Funct. Mater.* **2009**, *19*, 2467–2473.
3. Lee, S.-K.; Park, H. S.; Yi, G.-R.; Moon, J. H.; Yang, S.-M. Holographic Fabrication of Microstructures with Internal Nanopatterns Using Microprism Arrays. *Angew. Chem., Int. Ed.* **2009**, *48*, 7000–7005.
4. Zeng, H. B.; Xu, X. J.; Bando, Y.; Gautam, U. K.; Zhai, T. Y.; Fang, X. S.; Liu, B. D.; Golberg, D. Template Deformation-Tailored ZnO Nanorod/Nanowire Arrays: Full Growth Control and Optimization of Field-Emission. *Adv. Funct. Mater.* **2009**, *19*, 3165–3172.
5. Li, Y.; Sasaki, T.; Shimizu, Y.; Koshizaki, N. A Hierarchically Ordered TiO_2 Hemispherical Particle Array with Hexagonal-Non-Close-Packed Tops: Synthesis and Stable Superhydrophilicity without UV Irradiation. *Small* **2008**, *4*, 2286–2291.
6. Ye, C. H.; Zhang, L. D.; Fang, X. S.; Wang, Y. H.; Yan, P.; Zhao, J. W. Hierarchical Structure: Silicon Nanowires Standing on Silica Microwires. *Adv. Mater.* **2004**, *16*, 1019–1023.
7. Lao, J. Y.; Wen, J. G.; Ren, Z. F. Hierarchical ZnO Nanostructures. *Nano Lett.* **2002**, *2*, 1287–1291.
8. Gao, P. X.; Ding, Y.; Wang, Z. L. Crystallographic Orientation−Aligned ZnO Nanorods Grown by a Tin Catalyst. *Nano Lett.* **2003**, *3*, 1315–1320.
9. Ye, L.; Guo, W.; Yang, Y.; Du, Y.; Xie, Y. Directing the Architecture of Various MoS_2 Hierarchical Hollow Cages through the Controllable Synthesis of Surfactant/Molybdate Composite Precursors. *Chem. Mater.* **2007**, *19*, 6331–6337.
10. Cho, S. O.; Lee, E. J.; Lee, H. M.; Kim, J. G.; Kim, Y. J. Controlled Synthesis of Abundantly Branched, Hierarchical Nanotrees by Electron Irradiation of Polymers. *Adv. Mater.* **2006**, *18*, 60–65.
11. Wallraff, G. M.; Hinsberg, W. D. Lithographic Imaging Techniques for the Formation of Nanoscopic Features. *Chem. Rev.* **1999**, *99*, 1801–1822.
12. Smith, H. I.; Schattenburg, M. L. X-ray Lithography, from 500 to 30 nm: X-ray Nanolithography. *IBM J. Res. Dev.* **1993**, *37*, 319–330.
13. Stroscio, J. A.; Eigler, D. M. Atomic and Molecular Manipulation with the Scanning Tunneling Microscope. *Science* **1991**, *254*, 1319–1326.
14. Liu, G.-Y.; Xu, S.; Qian, Y. Nanofabrication of Self-Assembled Monolayers Using Scanning Probe Lithography. *Acc. Chem. Res.* **2000**, *33*, 457–466.
15. Gao, L.; McCarthy, T. J. The "Lotus Effect" Explained: Two Reasons Why Two Length Scales of Topography Are Important. *Langmuir* **2006**, *22*, 2966–2967.
16. Yang, S.-M.; Jang, S. G.; Choi, D.-G.; Kim, S.; Yu, H. K. Nanomachining by Colloidal Lithography. *Small* **2006**, *2*, 458–475.
17. Zhang, G.; Wang, D. Colloidal Lithography−The Art of Nanochemical Patterning. *Chem. Asian J.* **2008**, *4*, 236–245.

18. Li, Y.; Cai, W. P.; Duan, G. T. Ordered Micro/Nanostructured Arrays Based on the Monolayer Colloidal Crystals. *Chem. Mater.* **2008**, *20*, 615–624.
19. Chen, X.; Chen, Z. M.; Fu, N.; Lu, G.; Yang., B. Versatile Nanopatterned Surfaces Generated *via* Three-Dimensional Colloidal Crystals. *Adv. Mater.* **2003**, *15*, 1413–1417.
20. Jiang, P.; McFarland, M. J. Large-Scale Fabrication of Wafer-Size Colloidal Crystals, Macroporous Polymers and Nanocomposites by Spin-Coating. *J. Am. Chem. Soc.* **2004**, *126*, 13778–13786.
21. Haynes, C. L.; van Duyne, R. P. Nanosphere Lithography: A Versatile Nanofabrication Tool for Studies of Size-Dependent Nanoparticle Optics. *J. Phys. Chem. B* **2001**, *105*, 5599–5611.
22. Qi, L. M. Colloidal Chemical Approaches to Inorganic Micro- and Nanostructures with Controlled Morphologies and Patterns. *Coord. Chem. Rev.* **2010**, *254*, 1054–1071.
23. Li, Y.; Koshizaki, N.; Cai, W. Periodic One-Dimensional Nanostructured Arrays Based on Colloidal Templates, Applications, and Devices. *Coord. Chem. Rev.* **2011**, *255*, 357–373.
24. Chen, J.-T.; Chen, D.; Russell, T. P. Fabrication of Hierarchical Structures by Wetting Porous Templates with Polymer Microspheres. *Langmuir* **2009**, *25*, 4331–4335.
25. Li, Y.; Huang, X. J.; Heo, S. H.; Li, C. C.; Choi, Y. K.; Cai, W. P.; Cho, S. O. Superhydrophobic Bionic Surfaces with Hierarchical Microsphere/SWCNT Composite Arrays. *Langmuir* **2007**, *23*, 2169–2174.
26. Li, Y.; Lee, E. J.; Cho, S. O. Superhydrophobic Coatings on Curved Surfaces Featuring Remarkable Supporting Force. *J. Phys. Chem. C* **2007**, *111*, 14813–14817.
27. Duan, G. T.; Cai, W. P.; Luo, Y. Y.; Li, Y.; Lei, Y. Hierarchical Surface Rough Ordered Au Particle Arrays and Their Surface Enhanced Raman Scattering. *Appl. Phys. Lett.* **2006**, *89*, 181918.
28. Wang, D.; Möhwald, H. Rapid Fabrication of Binary Colloidal Crystals by Stepwise Spin-Coating. *Adv. Mater.* **2004**, *16*, 244–247.
29. Velikov, K. P.; Christova, C. G.; A. Dullens, R. P.; van Blaaderen, A. Layer-by-layer Growth of Binary Colloid Crystals. *Science* **2002**, *296*, 106–109.
30. Kim, M. H.; Im, S. H.; Park, O. O. Fabrication and Structural Analysis of Binary Colloidal Crystals with Two-Dimensional Superlattices. *Adv. Mater.* **2005**, *17*, 2501–2505.
31. Wang, J.; Li, Q.; Knoll, W.; Jonas, U. Preparation of Multilayered Trimodal Colloid Crystals and Binary Inverse Opals. *J. Am. Chem. Soc.* **2006**, *128*, 15606–15607.
32. Wang, J.; Ahl, S.; Li, Q.; Kreiter, M.; Neumann, T.; Burkert, K.; Knoll, W.; Jonas, U. Structural and Optical Characterization of 3D Binary Colloidal Crystal and Inverse Opal Films Prepared by Direct Codeposition. *J. Mater. Chem.* **2008**, *18*, 981–988.
33. Wang, L.; Wan, Y.; Li, Y.; Cai, Z.; Li, H.-L.; Zhao, X. S.; Li, Q. Binary Colloidal Crystals Fabricated with a Horizontal Deposition Method. *Langmuir* **2009**, *25*, 6753–6759.
34. Liu, J.; Cai, Y.; Deng, Y.; Sun, Z.; Gu, D.; Tu, B.; Zhao, D. Magnetic 3-D Ordered Macroporous Silica Templated from Binary Colloidal Crystals and Its Application for Effective Removal of Microcystin. *Microporous Mesoporous Mater.* **2010**, *130*, 26–31.
35. Kitaev, V.; Ozin, G. A. Self-Assembled Surface Patterns of Binary Colloidal Crystals. *Adv. Mater.* **2003**, *15*, 75–78.
36. Vermolen, E. C. M.; Kuijk, A.; Filion, L. C.; Hermes, M.; Thijssen, J. H. J.; Dijkstra, M.; van Blaaderen, A. Fabrication of Large Binary Colloidal Crystals with a NaCl Structure. *Proc. Natl. Acad. Sci. U.S.A.* **2009**, *106*, 16063–16067.
37. Yu, J.; Yan, Q.; Shen, D. Co-self-assembly of Binary Colloidal Crystals at the Air-water Interface. *Appl. Mater. Interfaces* **2010**, *2*, 1922–1926.
38. Vogel, N.; de Viguerie, L.; Jonas, U.; Landfester, K.; Weiss, C. K. Wafer-Scale Fabrication of Ordered Binary Colloidal Monolayers with Adjustable Stoichiometries. *Adv. Funct. Mater.* **2011**, *21*, 3064–3073.
39. Wenzel, R. N. Surface Roughness and Contact Angle. *J. Phys. Colloid Chem.* **1949**, *53*, 1446–1467.
40. Kosiorek, A.; Kandulski, W.; Glaczynska, H.; Giersig, M. Fabrication of Nanoscale Rings, Dots, and Rods by Combining Shadow Nanosphere Lithography and Annealed Polystyrene Nanosphere Masks. *Small* **2005**, *1*, 439–444.
41. Rybczynski, J.; Ebels, U.; Giersig, M. Large-scale, 2D Arrays of Magnetic Nanoparticles. *Colloids Surf., A* **2003**, *219*, 1–6.
42. Retsch, M.; Zhou, Z.; Rivera, S.; Jonas, U.; Kappl, M.; Zhao, X. S.; Li, Q. Fabrication of Large Area, Transferable Colloidal Monolayers Utilizing Self-Assembly at the Air/Water Interface. *Macromol. Chem. Phys.* **2009**, *210*, 230–241.
43. Dinsmore, A. D.; Hsu, M. F.; Nikolaides, M. G.; Marquez, M.; Bausch, A. R.; Weitz, D. A. Colloidosomes: Selectively Permeable Capsules Composed of Colloidal Particles. *Science* **2002**, *298*, 1006–1009.
44. Li, Y.; Cai, W.; Cao, B.; Duan, G.; Li, C.; Sun, F.; Zeng, H. Morphology-Controlled 2D Ordered Arrays by Heating-Induced Deformation of 2D Colloidal Monolayer. *J. Mater. Chem.* **2006**, *16*, 609–612.
45. Li, Y.; Lee, E. J.; Cai, W.; Kim, K. Y.; Cho, S. O. Unconventional Method for Morphology-Controlled Carbonaceous Nanoarrays Based on Electron Irradiation of a Polystyrene Colloidal Monolayer. *ACS Nano* **2008**, *2*, 1108–1112.
46. Li, Y.; Sasaki, T.; Shimizu, Y.; Koshizaki, N. Hexagonal-Close-Packed, Hierarchical Amorphous TiO_2 Nanocolumn Arrays: Transferability, Enhanced Photocatalytic Activity, and Superamphiphilicity without UV Irradiation. *J. Am. Chem. Soc.* **2008**, *130*, 14755–14762.
47. Li, Y.; Koshizaki, N.; Shimizu, Y.; Li, L.; Gao, S.; Sasaki, T. Unconventional Lithography for Hierarchical Micro-/Nanostructure Arrays with Well-Aligned 1D Crystalline Nanostructures: Design and Creation Based on the Colloidal Monolayer. *ACS Appl. Mater. Interfaces* **2009**, *1*, 2580–2585.
48. Gao, S.; Koshizaki, N.; Li, Y.; Li, L. Unique Hexagonal Non-close-packed Arrays of Alumina Obtained by Plasma Etching/Deposition with Catalytic Performance. *J. Mater. Chem.* **2011**, *21*, 2087–2090.
49. Cavallini, M.; Stoliar, P.; Moulin, J. F.; Surin, M.; Leclère, P.; Lazzaroni, R.; Breiby, D. W.; Andreasen, J. W.; Nielsen, M. M.; Sonar, P.; Grimsdale, A. C.; Müllen, K.; Biscarini, F. Field-Effect Transistors Based on Self-Organized Molecular Nanostripes. *Nano Lett.* **2005**, *5*, 2422–2425.
50. Wang, R; Hashimoto, K.; Fujishima, A; Chikuni, M.; Kojima, E.; Kitamura, A.; *et al.* Light-Induced Amphiphilic Surfaces. *Nature* **1997**, *388*, 431–432.
51. Wang, R.; Hashimoto, K.; Fujishima, A.; Chikuni, M.; Kojima, E.; Kitamura, A.; Shimohigoshi, M.; Watanabe, T. Photogeneration of Highly Amphiphilic TiO_2 Surfaces. *Adv. Mater.* **1998**, *10*, 135–138.
52. Xiong, Y.; Mclellan, J. M.; Chen, J.; Yin, Y.; Li, Z. Y.; Xia, Y. Kinetically Controlled Synthesis of Triangular and Hexagonal Nanoplates of Palladium and Their SPR/SERS Properties. *J. Am. Chem. Soc.* **2005**, *127*, 17118–17127.
53. Kim, H.; Kosuda, K. M.; Van Duyne, R. P.; Stair, P. C. Resonance Raman and Surface- and Tip-Enhanced Raman Spectroscopy to Study Solid Catalysts and Heterogeneous Catalytic Reactions. *Chem. Soc. Rev.* **2010**, *39*, 4820–4844.
54. Duan, G. T.; Cai, W. P.; Luo, Y. Y.; Li, Z. G.; Li, Y. Electrochemically Induced Flowerlike Gold Nanoarchitectures and Their Strong Surface-Enhanced Raman Scattering Effect. *Appl. Phys. Lett.* **2006**, *89*, 211905.
55. Nie, S. M.; Emory, S. R. Probing Single Molecules and Single Nanoparticles by Surface-Enhanced Raman Scattering. *Science* **1997**, *275*, 1102–1106.
56. Li, S.; Pedano, M.; Chang, S.-H.; Mirkin, C. A.; Schatz, G. C. Gap Structure Effects on SERS Intensities for Gold Gapped-Rods. *Nano Lett.* **2010**, *10*, 1722–1727.
57. Gaponenko, S. G. Effects of Photon Density of States on Raman Scattering in Mesoscopic Structures. *Phys. Rev. B.* **2002**, *65* 140303(R).
58. Zuev, V. S.; Frantsesson, A. V.; Gao, J.; Eden, J. G. Enhancement of Raman Scattering for an Atom or Molecule near a

Metal Nanocylinder: Quantum Theory of Spontaneous Emission and Coupling to Surface Plasmon Modes. *J. Chem. Phys.* **2005**, *122*, 214726.
59. Duan, G. T.; Cai, W. P.; Luo, Y. Y.; Li, Y.; Lei, Y. Hierarchical Surface Rough Ordered Au Particle Arrays and Their Surface Enhanced Raman Scattering. *Appl. Phys. Lett.* **2006**, *89*, 181918.